

# Modelling an ideal gas using a molecular dynamics simulation

University College London

**Abstract**—This report examines the behaviour of an ideal gas that has been simulated in Python. The simulation exhibits the expected relations between state variables such as a positive correlation between pressure and the number of gas particles in the box -  $r=0.93$  - as well as a positive correlation between the piston's average height and the gas's temperature  $r=0.75$  (where  $r$  is the Pearson correlation coefficient). The results are supported by thermodynamic theory and verifies the validity of the simulation.

## I. INTRODUCTION

THE problem that our investigation is addressing is whether the relevant thermodynamic theory agrees with the results that our molecular dynamics simulation has uncovered. Our understanding of the motion of gas arises from statistical mechanics [1] where a system's microstates (a description of the system where the variables are specified) match the macrostate of the system (a collection of individual microstates that are distinguished by a common property of the system such as its temperature).

The behaviour of gas particles has been studied extensively since the mid-18th century and has led to technological advancements in machinery and engineering which propelled the industrial revolution. Practically, the discoveries that the study of thermodynamics has uncovered has undoubtedly improved our quality of life namely the development of engines and it has also accelerated our understanding of nature. Without such a theory we may not understand the physics behind stars and their lifecycle, nor would we be able to model how the behaviour of air molecules enable aircrafts to traverse the sky. Overall thermodynamic theory is essential to our understanding of the universe which is why it is important to understand the process of simulating thermodynamic scenarios.

## II. THEORY

In the simulation, the particle's velocities are described by the Maxwell-Boltzmann distribution in three dimensions. This distribution can be motivated from statistical mechanics [1] where one can coarse grain a system so that there are a finite number of ways to distribute gas particles in a container. The multiplicity of microstates (which is the total number of microstates denoted as  $\Omega(Q, N)$ , where  $Q$  represents the number of particles and  $N$  represents the number of positions a particle could occupy) can be expressed as:

$$\Omega(Q, N) = \frac{N!}{(N - Q)!Q!} \quad (1)$$

The probability of a system being in a specified microstate is therefore proportional to  $\Omega$  as it is assumed that every microstate has an equal probability of being prevalent. For large values of  $N$  and  $Q$  the Stirling approximation can be utilized to approximate large factorials as:

$$\ln m! = m \ln m - m; m \gg 1 \quad (2)$$

This theory can be applied to a canonical ensemble which is a system that can exchange energy with its environment. Adapting the multiplicity term that has been defined above, one can show that the probability that a macrostate possesses an energy  $E$  is as follows:

$$P(E) = \frac{\Omega(E)e^{-\beta E}}{Z} \quad (3)$$

Where  $\beta = \frac{1}{k_B T}$  and  $Z$  is the canonical partition function:

$$Z = \sum_E \Omega(E)e^{-\beta E} \quad (4)$$

The ideal gas assumptions are as follows [2]: gases contain particles which exhibit Brownian motion with a velocities distributed according to the Maxwell-Boltzmann distribution, the volume of the box occupied by the particles themselves is negligible compared to the box's volume, the particles act as spheres, pressure arises from collisions between the particles and the box's walls, all collisions are assumed to be perfectly elastic and the intermolecular forces between the particles are ignored.

The ideal gas law [2]:

$$pV = Nk_B T \quad (5)$$

(where  $k_B$  has been set to unity) describes the behaviour between the following state variables: pressure, volume, the number of particles and temperature. This equation provides a framework of how one can describe the effect that changing a state variable has on the system.

From the ideal gas law, the following relation for a particle's kinetic energy and thermal energy can be established [1]:

$$\frac{1}{2}m\langle v^2 \rangle = \frac{3}{2}k_B T \quad (6)$$

The probability of each particle possessing a particular velocity is weighted by the Boltzmann factor ( $e^{-\beta E}$ ) and the velocity microstates are assumed to be found with equal

density across the spatial dimensions. Following on from this, one can arrive at the Maxwell-Boltzmann distribution in three dimensions:

$$P(v)dv \propto v^2 e^{-\beta \frac{1}{2}mv^2} dv \quad (7)$$

Or more formally written:

$$P(v)dv = 4\pi v^2 \left( \frac{m}{2\pi k_B T} \right)^{\frac{3}{2}} e^{-\frac{mv^2}{2k_B T}} dv \quad (8)$$

### III. METHODOLOGY

#### A. Initial set-up

The particles' initial positions were randomised to be within the limits of the box which in the coordinates that we used were  $0 > x_0 > w$ ,  $0 > y_0 > h$ ,  $0 > z_0 > d$  (h-height, w-width and d-depth). In the case of the piston height function the initial maximum possible height was determined by h whereas the piston's starting height was the parameter  $h_0$  to ensure that all the particles are within the box's boundaries.

Initially, we were modelling in two dimensions, so we were able to implement inverse transform sampling [3] to map the particles' velocities to the 2D Maxwell-Boltzmann distribution:

$$P(v)dv = \frac{mv}{k_B T} e^{-\frac{mv^2}{2k_B T}} dv \quad (9)$$

The inverse of the probability density function's integral is:

$$v = \sqrt{\log U \times 2 \sqrt{\frac{k_B T}{m}}} \quad (10)$$

Where U is a pseudo-random number between zero and unity. Using this relation, we were able to fit the particles' initial velocities to the distribution.

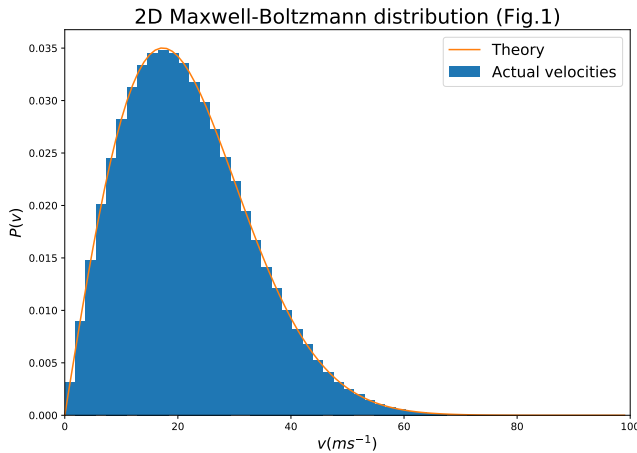


Fig. 1: 2D distribution of velocities and probability of a particle possessing that velocity; T = 300k and particle mass = 1kg.

We were unable to use the same method for the three-dimensional Maxwell-Boltzmann distribution because its integral is not invertible, so we used `maxwell.ppf` from `scipy.stats` and scaled it with  $\sqrt{\frac{k_B T}{m}}$  in order to fit the particles' initial velocities in three dimensions.

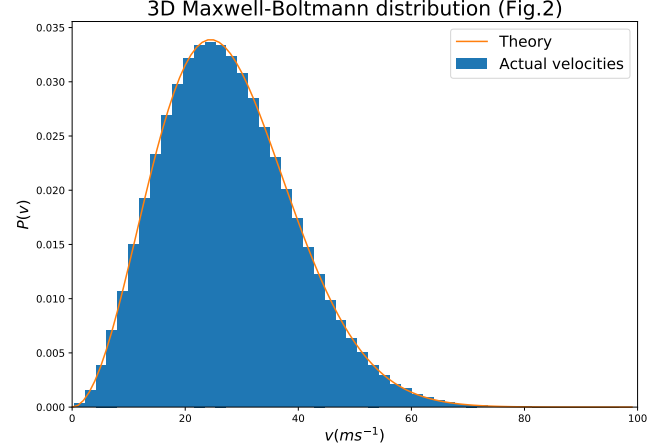


Fig. 2: 3D distribution of velocities and probability of a particle possessing that velocity; T = 300k and particle mass = 1kg.

This curve predicts the equilibrium velocity distribution that the gas's constituent particles will tend to as they reach equilibrium. As the gas particles in the simulation do not interact with each other we have chosen to initialize the particles' velocities using this distribution (with randomised components) as the magnitude of the particles' velocities are invariant in the simulation.

#### B. Particle propagation

To allow the system to evolve, a timestep of  $\delta t = 1 \times 10^{-5} s$  was set and the time in which the system evolves is specified by an input parameter 'total time'. As the simulation progresses, each of the three position components is updated by an amount:

$$\mathbf{r}_{\text{next}} = \mathbf{r}_0 + \mathbf{v} \times \delta t \quad (11)$$

where  $\mathbf{r}_0$  are the particles' coordinates at the previous timestep. The equation of motion is then looped over all 'N' particles for  $\frac{\text{totaltime}}{\delta t}$  many steps. After each particle's position change, the function sets  $\mathbf{r}_0 = \mathbf{r}_{\text{next}}$ , as the particles' starting position for the next timestep must now be updated.

At the box's boundaries the collisions are assumed to be perfectly elastic, so the particles' kinetic energies do not change upon a collision as the walls are completely stationary. Therefore if a particle's position is within a tolerance of  $1 \times 10^{-10} m$  from any of the input dimensions h, w or d in x, y or z respectively, or if x, y or z approach zero then the boundaries are at zero plus the tolerance value, the component

of velocity perpendicular to the plane of the boundary is reversed. For example, if a particle's horizontal component satisfies:  $x_{\text{next}} > w - \text{tol}$ , then  $\mathbf{u} = -\mathbf{u}$  (shown by Fig.3).

Snapshots of particle collision (Fig.3)

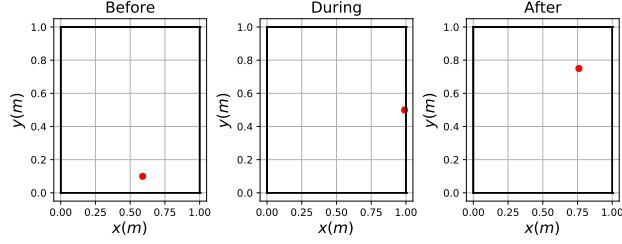


Fig. 3: Three stages of a particle collision with a wall in a test simulation.

These equations of motion and boundary conditions allowed us to update a list of position coordinates for each particle and plot 'N' trajectories. This approach is how the simulation was able to plot the paths of multiple particles as displayed in Fig.4.

Particle trajectories (Fig.4)

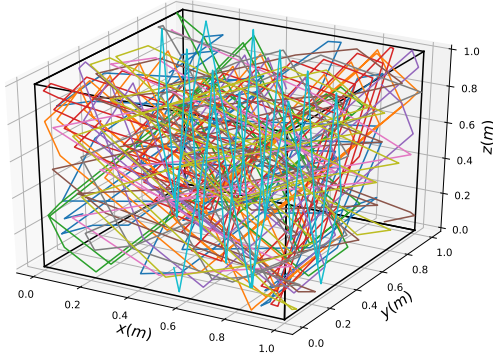


Fig. 4: Paths of 10 different particles;  $T = 300\text{k}$ , particle mass =  $1\text{kg}$ , volume =  $1\text{m}^3$  and total time =  $1\text{s}$ . Note different colours represent that paths of different particles.

### C. Pressure calculation

The next step of the investigation was to use the position functions to calculate the pressure of the gas on the container's boundaries. To do this, the position function counted how many times each particle collided with one of the six walls and summed each particle's contribution to the total pressure. This calculation was performed using Newton's second law of motion:

$$\mathbf{F} = \frac{d\mathbf{p}}{dt} \quad (12)$$

for which, when the impulse of a particle is considered and the force is manipulated to show the pressure of a collision, the resulting expression is [1]:

$$P = \left( \frac{2m\mathbf{v}}{\delta t} \right) \frac{1}{A} \quad (13)$$

where 'P' is the pressure exerted, 'A' corresponds to the area of the wall that the particle has collided with and ' $\delta t$ ' is the total time elapsed. We wanted to take an average of the pressure over the simulation time span, so we divided each pressure contribution by 'total time'.

### D. Piston propagation

The final amendment to our function was to add the piston's height to the simulation. The 'piston height3D' function takes an extra input  $h_0$  which is the initial height of the piston above the bottom of the box. It is intended that  $h_0 > h$  to avoid any gas particles potentially escaping the box. The particles are unable to go higher than the piston as the same boundary conditions are enforced there as at the box's walls.

The piston's motion was modelled to fall under the influence of gravity:

$$\mathbf{h}_{\text{next}} = \mathbf{h}_0 + \mathbf{v}\delta t + \frac{1}{2}g\delta t^2 \quad (14)$$

where  $g = -9.81\text{ms}^{-2}$ . When a particle collides with the piston, the particles' velocity component which is perpendicular to the piston reverses (the same as wall collisions) but due to the conservation of linear momentum [4] the piston's velocity changes by:

$$\delta\mathbf{v} = \frac{2m_{\text{gas}}|\mathbf{v}_{\text{gas}}|}{m_{\text{piston}} + m_{\text{gas}}} \quad (15)$$

which consequently leads to the piston's next height update to be [3]:

$$\mathbf{h}_{\text{next}} = \mathbf{h}_0 + \delta t\mathbf{v}_{\text{next}} + (\delta t)^2 \left( \frac{2m_{\text{gas}}|\mathbf{v}_{\text{gas}}|}{2m_{\text{gas}}\delta t} \right) \quad (16)$$

This expression shows how each discrete impact changes the direction of the piston and suggests that particles with greater velocities and greater masses will have more of an effect on the height of the piston.

#### IV. RESULTS

To verify the ideal gas equations, we will first present the relations between the pressure exerted on a box with fixed dimensions (no piston). The unit of pressure (which has been denoted as ‘standard unit’) is slightly ambiguous as we have set  $k_B = 1$  and the particle mass is 1kg which is unrealistic. Despite this, the plots are still able to show how the pressure changes relatively due to a change in the gas’s state.

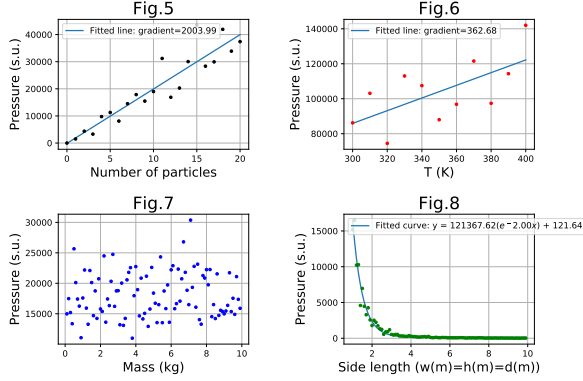


Fig. 5: **Pressure against number of particles**;  $T = 300K$ , particle mass = 1kg, volume =  $1m^3$  and total time = 1s.

Fig. 6: **Pressure against temperature of gas**; particle mass = 1kg, volume =  $1m^3$ ,  $N = 50$  and total time = 1s.

Fig. 7: **Pressure against particle mass**;  $T = 300K$ , volume =  $1m^3$ ,  $N=10$  and total time = 1s.

Fig. 8: **Pressure against side length**;  $T = 300K$ , particle mass = 1kg,  $N = 10$  and total time = 1s.

Using `np.polyfit` and `pearsonr` from `scipy.stats` the gradients of the best fit line and correlations of the data were determined. The gradient of the best fit line in Fig.5 was determined to be  $2003.99 \pm 181.04$  s.u. and the Pearson correlation test yielded a strong positive correlation of  $r = 0.93$ . The gradient of the best fit line in Fig.6 was determined to be  $362.68 \pm 142.77$  s.u./K and the correlation test resulted in a weak positive correlation of  $r = 0.64$ . As Fig.7 showed no clear correlation, we were unable to analyse any trends here. Fig.8 was modelled using `scipy.optimize` and was fitted to a curve  $y = 121367.62e^{-2x} + 121.64$  where the error in the gradient was determined to be  $\pm 0.08J^{-1}$  and the correlation between the pressure and the volume’s inverse was strongly positive;  $r = 0.89$ .

As well as this, we have plotted the path of the piston’s height as it compresses the gas and have included snapshots of the gas’s spatial dimensions.

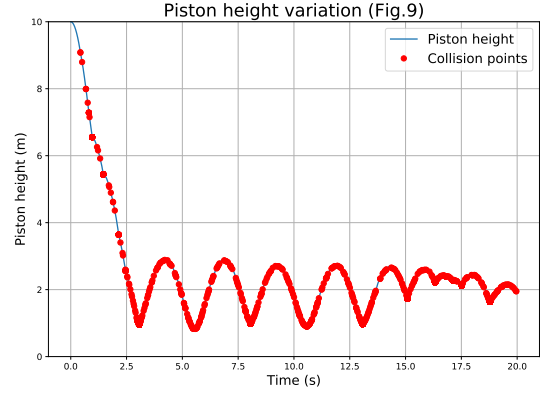


Fig. 9: **Piston height against time**;  $T = 500K$ , particle mass = 1kg, piston mass = 100kg, initial volume =  $1m^3$ , piston’s initial height = 10m,  $N = 10$  and total time = 20s.

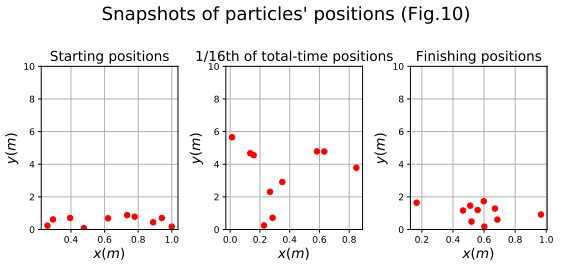


Fig. 10: **Position snapshots in x-y plane at start, one sixteenth of the total-time positions and the final positions**. Note the one sixteenth plot may seem like an ambiguous time to plot but we chose it to illustrate how the particles initially move upwards towards the piston. Also, these plots are in the x-y plane for clarity.

We have also varied the number of particles in the gas and observed the effects on the piston’s fluctuations.

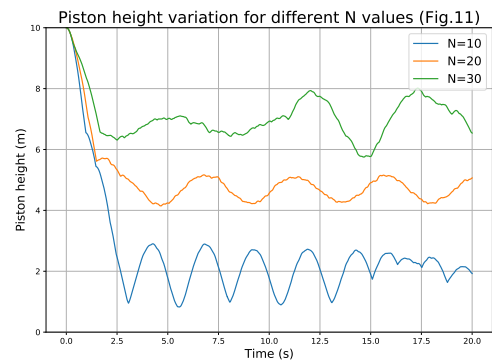


Fig. 11: **Plot of piston height against time for different values of N**;  $T = 500K$ , particle mass = 1kg, piston mass = 100kg, initial volume =  $1m^3$ , piston’s initial height = 10m and total time = 20s. Note the data used for ‘N=10’ is the same data as displayed in Fig.9.

As well as this, we have explored how the piston's height changes for longer simulation times.

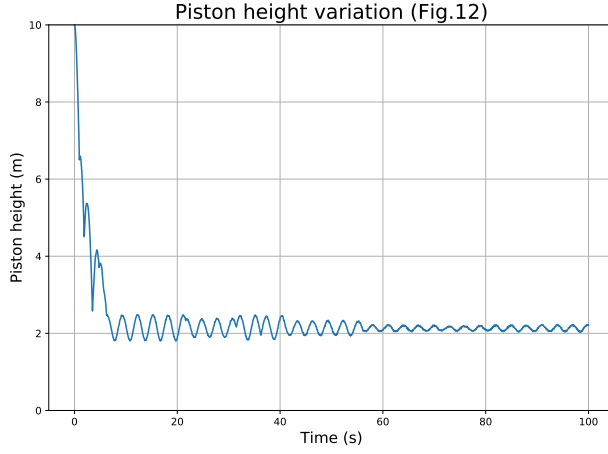


Fig. 12: **Piston height against time;**  $T = 500\text{K}$ , particle mass =  $1\text{kg}$ , piston mass =  $100\text{kg}$ , initial volume =  $1\text{m}^3$ , piston's initial height =  $10\text{m}$ ,  $N = 10$  and total time =  $100\text{s}$ .

We have also explored how the average height of the piston changes as the temperature of the gas is varied.

Piston's average height against temperature of particles (Fig.13)

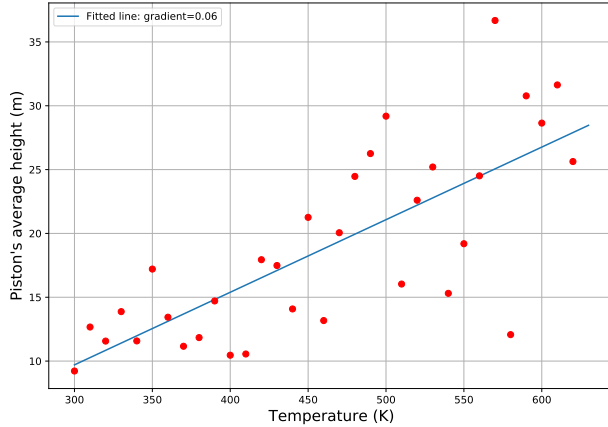


Fig. 13: **Plot of piston's average height against temperature of gas particles;** particle mass =  $1\text{kg}$ , piston mass =  $100\text{kg}$ , initial volume =  $9.5\text{m}^3$  (where the initial maximum possible gas particle position is at  $9.5\text{m}$ ), piston's initial height =  $10\text{m}$ ,  $N=50$  and total time =  $5\text{s}$  Note that as we are computing 50 particles we had to only consider a short time span (so the computational time isn't excessive) of  $5\text{s}$  so we have made the maximum initial height of the gas particles  $9.5\text{m}$  to ensure the piston and particles can interact within the time span.

The gradient of this line of best fit is  $0.060 \pm 0.009\text{mK}^{-1}$  and the correlation is strongly positive with a Pearson correlation of  $r = 0.75$ .

Moreover, the relation between the piston's average height and the mass ratio between the piston and the total particle mass has been explored.

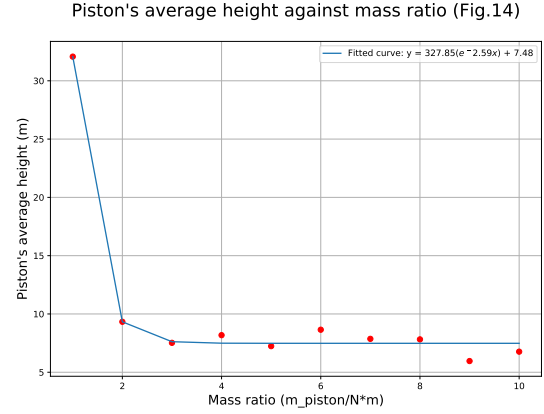


Fig. 14: **Plot of piston's average height against mass ratio of piston and sum of particle mass  $\frac{m_{\text{piston}}}{m_{\text{gas}}}$ ;**  $T = 600\text{K}$ , particle mass =  $1\text{kg}$ , initial volume =  $9.5\text{m}^3$  (where the initial maximum possible gas particle position is at  $9.5\text{m}$ ), piston's initial height =  $10\text{m}$ ,  $N = 50$ , total time =  $5\text{s}$ .

The fitted curve's equation is  $y = 327.85e^{-2.59x} + 7.48$  and the gradient's error is  $\pm 0.49\text{m}^{-1}$ . As well as this, the correlation between the average height and the mass ratio's inverse is  $r = 0.92$ .

## V. DISCUSSION

Physically, Fig.5 has a positive correlation of  $r = 0.93$  because more gas particles collide with the box's walls, consequently causing more collisions to occur in a given interval. As well as this, the ideal gas law suggests that  $p \propto N$  which is observed in this simulation. However, the observed gradient does not match the expected gradient that the ideal gas equation suggests which is  $\frac{k_B T}{V}$  ( $300\text{ s.u.}$ ). This means that Fig.5's gradient is a factor of  $\sim 6\frac{2}{3}$  off the predicted gradient. This discrepancy may be due to the computational limitations as we were unable to feasibly simulate a realistic number of particles without incurring an extensive run-time. Despite this the relative uncertainty in the data of  $\sim 10\%$  is encouraging and suggests that the simulation is accurate in terms of the trend that has been documented, considering the smaller number of particles.

The plot of pressure against temperature (Fig.6) demonstrates a weak positive correlation of  $r = 0.64$ . The positive correlation was expected as the gas particles have a greater average velocity  $\left(s_{\text{avg}} = \sqrt{\frac{2k_B T}{m}}\right)$  so there will be more collisions per second within the box and each collision will impart a greater force on the box's boundaries. Also, as the ideal gas law shows,  $p \propto T$  but as before with Fig.5 there is a discrepancy in the gradient, in this case of  $\sim 5$  for the same reasons that were previously explored. The relative uncertainty in this gradient is  $\sim 40\%$  which suggests that the simulation

may require a greater number of particles to reduce this error as the velocity distribution for 50 particles may be uneven and not truly represent the Maxwell-Boltzmann distribution.

Fig.7 shows no evident correlation between particle mass and pressure. One may expect to find a positive correlation here as  $p$  (from the impulse equation) but the average particle speed also depends on the mass:  $s_{avg} \propto \frac{1}{\sqrt{m}}$ . This means overall that increasing the particle mass may increase the force per collision but it will also reduce the number of collisions that occur. Therefore, it is entirely plausible that there is no correlation between particle mass and pressure.

Changing the side length of the box (Fig.8) has an evident effect on the pressure exerted by the gas. The general direction of the plots follows a  $y = \frac{1}{x^3}$  curve as the volume is the cube of the side length and  $p \propto \frac{1}{V}$ . The fitted curve  $y = 121367.62e^{-2x} + 121.64$  effectively maps the curve's path and has a smaller absolute uncertainty in its gradient of  $\pm 0.08J^{-1}$  as there is a strong positive correlation between the pressure and the volume's inverse of  $r = 0.89$ . Physically this decrease in pressure as the side length increases is because the frequency of collisions will decrease as the boundaries are further apart causing the particles to have more distance to cover between collisions.

Due to the relatively small number of particles that the simulation models, the piston's height will fluctuate due to the irregular collisions. As you can see from Fig.9 the piston initially falls due to gravitational acceleration. The red points on the piston height curve indicate when there has been a collision with a gas particle. After around three seconds the piston's height begins to oscillate and converge on a height of 2 metres. This is because the gas has become increasingly pressurised due to the box's decreasing volume. Therefore, the upwards force of the gas and the downwards force of gravity begin to balance out and converge on a definite height. As you can see from Fig.10, the particles' spatial distribution changes from the initial volume of  $1m^3$  (as this is a specified parameter) to colliding with the piston as it initially falls, to finally occupying a volume of  $\sim 2m^3$  as the piston is reaching equilibrium.

As you can see from Fig.11 the piston's convergence height increases as the number of particles in the box increases for the same reasons as discussed previously (Fig.5). Also, the frequency of fluctuations tends to decrease as the number of particles increase. This suggests that the piston reaches equilibrium in less time if there are more particles in the box. Physically this effect may be a consequence of there being more force on the piston from the gas, which subsequently allows the piston to reach equilibrium faster as the forces are closer to balancing out. This is because there is a greater opposition to the initially dominant force of gravity pulling the piston downwards. However, as the number of particles is sparse and their individual mass is unrealistically large, there will always be some fluctuations as each discrete impact will

inflict a large force on the piston causing its height to change accordingly.

As Fig.12 indicates, larger simulation times allow the amplitude of the piston's oscillations to decrease and begin to converge at a definite height. The curve that is observed is analogous to a forced oscillator exhibiting simple harmonic motion. At  $\sim 60s$  the oscillator's amplitude decreases which may suggest that the simulation has a critical time, after which the volume of the gas becomes more precisely defined. This implies that one must run the simulation for a longer time in order to allow convergence to occur but due to the computational limits of the simulation, a large number of particles and a large simulation time will result in an extensive running time.

As Fig.13 suggests there is a positive correlation,  $r = 0.75$  between the piston's average height and the temperature of the gas. This figure is analogous to Fig.6 as the positive correlation in both figures is due to the increase in pressure which arises from more frequent collisions and greater impulses from each collision due to an increase in the average particle velocity. Increasing the temperature would consequently increase the pressure of the gas which therefore increases the average piston height. This is because there is a greater upwards force from the gas particles which counteracts the piston's weight and leads to a height convergence at a higher value. The plots of piston height against time for the data points shown in Fig.13 would resemble the paths presented in Fig.11 and would converge over a longer period as shown in Fig.12. The small error in the fitted line's gradient,  $0.060 \pm 0.009mK^{-1}$ , suggests that the fitted line accurately maps the average piston height's variation as the gas's temperature is increased.

Fig.14 shows the effect of changing the ratio between the piston's mass and the sum of the individual particle masses on the piston's average height. The relation between these quantities resemble a  $y = \frac{1}{x}$  curve with an asymptotic region around 7m. As expected, the average height of the piston when the piston's mass is equal to the combined particle mass (mass ratio = 1) results in an exceedingly large average height as the gravitational force of the piston is significantly reduced and each discrete impact causes the piston to experience a greater change in velocity. As the mass ratio increases to 3, the average height begins to become invariant upon further increases to the mass of the piston. This may be due to a limitation in the simulation as increasing the total time that was being averaged across above 5 seconds would result in extended running times. However, from this figure one can observe that the average piston height converges as the piston's mass increases with respect to the sum of the particle mass. Physically this may be a consequence of the gas becoming in-compressible as the pressure exerted by the gas particles cannot be overcome by increasing the piston's mass. There is also a strong positive correlation between the piston's average height and the mass ratio's inverse of  $r = 0.92$ . This supports the theory that the two quantities are inversely proportional. As well as this, the fitted curve,  $y = 327.85e^{-2.59x} + 7.48$

has approximately a  $\sim 20\%$  relative uncertainty as the error is  $\pm 0.49m^{-1}$  which suggests that the fitted curve appropriately represents the data.

## VI. CONCLUSION

To conclude, our simulation has recovered many of the basic relations between thermodynamic state variables. Although, there are some discrepancies between the gradients of the pressure plots and the theoretical predictions, we are satisfied with the correlations that the simulations have uncovered as they agree with thermodynamic theory and can be explained comprehensibly.

To make the simulation more accurate, the boundary conditions could have been more realistic by including a coefficient of restitution when determining the rebound velocity. This could have depended on the box's material and would have made the simulation more realistic. As well as this, we could have incorporated the Lennard-Jones potential and allowed the particles to repel each other. Also, the simulation is not valid for all temperatures as it is evident from statistical mechanics [1] that Fermi-Dirac statistics and Bose-Einstein statistics are more prevalent in the limit of  $T \sim 0K$ . At these lower temperatures we could have included the effect of the particles' spins (fermions or bosons) and subsequently used the equations for Fermi-Dirac statistics and Bose-Einstein statistics in these limits and utilise the following partition functions:

$$\langle N \rangle^{(\epsilon)} = \frac{1}{e^{\beta(\epsilon - \mu)} \pm 1} \quad (17)$$

This quantum behaviour will come into effect when the gas's density is approximately the inverse cube of the thermal de Broglie wavelength [1]:  $\lambda_{th} = \frac{h}{\sqrt{2\pi m k_B T}}$  :

$$n_q = \lambda_{th}^{-3} \quad (18)$$

However, given the specification for the project these additional complications were deemed unnecessary, but it is important to acknowledge the simulation's limitations.

To further improve the accuracy and validity of the simulation we could have utilized 'np.where' when computing the boundary conditions within the functions. This would have undoubtedly reduced the running time of the functions and therefore the simulations would have been able to model with a more realistic number of particles. As well as this, we could have simulated beyond the critical time of 60 seconds when considering the piston's height variation. As well of this, we would have been able to feasibly consider the particle-particle collisions without dramatically increasing the computational time. This refinement would have made the simulation more accurate physically and would complete the ideal gas approximations (along with modelling gas particles as spheres). If we were able to do this project again, we would focus on making the functions more computationally efficient so we could refine our assumptions and save time when generating the plots.

## VII. REFERENCES

PHAS0024 Statistical Physics of Matter, Prof Bart Hoogenboom, 08/01/21 – [1]

Ideal gases and the ideal gas law:  $pV = nRT$ , Chemguide.co.uk, <https://www.chemguide.co.uk/physical/kt/idealgases.html> - [2]

Session 7 PHAS0030, Prof David Bowler, 2020/2021 – [3]

Collisions — Boundless Physics, Courses.lumenlearning.com, <https://courses.lumenlearning.com/boundless-physics/chapter/collisions/> - [4]